Rare Metal Materials and Engineering
Volume 50, Issue 12, December 2021
Available online at www.rmme.ac.cn

Science Press

Cite this article as: Shi Shuangxi, Fan Kai, Yang Sheng, et al. Microstructure Evolution and Mechanical Properties of Ti-55511 Alloy with Equiaxed and Lamellar Microstructures During Hot Rolling and Annealing[J]. Rare Metal Materials and Engineering, 2021, 50(12): 4296-4305.

ARTICLE

Microstructure Evolution and Mechanical Properties of Ti-55511 Alloy with Equiaxed and Lamellar Microstructures During Hot Rolling and Annealing

Shi Shuangxi[1], Fan Kai[2], Yang Sheng[2], Zhang Xiaoyong[1], Zhou Kechao[1]

[1] State Key Laboratory of Powder Metallurgy, Central South University, Changsha 410083, China; [2] Hunan Goldsky Titanium Industry Technology Co., Ltd, Changde 410007, China

Abstract: The equiaxed and lamellar microstructures of T-55511 alloy were obtained by different heat treatment routes. Microstructure evolution and mechanical properties of Ti-55511 alloy with equiaxed and lamellar microstructures during hot rolling and annealing were investigated by SEM, EBSD, TEM and tensile tests. The results show that equiaxed α phases are slightly deformed and β phase experiences dynamic recovery and dynamic recrystallization during 750 ºC rolling; whereas lamellar α phase is nearly distributed in parallel, some of which are partly fragmentized, and β phase merely undergoes dynamic recovery. Texture intensity of α phase increases remarkably in lamellar structure but slightly in equiaxed structure, while texture intensity of β phase decreases both in equiaxed and lamellar structure. In addition, the anisotropy of equiaxed structure is small while that of lamellar structure is obvious. When the rolled lamellar structure is annealed at 600 °C, texture intensities of α and β phase both decrease and the anisotropy of mechanical properties significantly decreases.

Key words: Ti-55511 alloy; dynamic recovery; dynamic recrystallization; microstructure evolution; texture

Near β titanium alloys such as Ti-55511 have been widely used to fabricate some key load-bearing components in aerospace industry due to their high specific strength, excellent corrosion resistance and good fracture toughness[1-4]. These excellent mechanical properties are closely related to the microstructure, such as content, size, distribution and morphology of α phase, which can be suitably controlled by thermomechanical processing[5,6]. A typical processing route for near β-titanium alloys involves a prior hot deformation and heat treatment in single β phase region to break ingot structure and form a transformed microstructure. Subsequently, a finishing hot deformation in the α+β region and heat treatment achieve the following objectives: the transformed microstructures are spheroidized to produce the desired microstructure, texture, and properties[7,8]. Therefore, understanding the relationship among microstructure evolution, texture evolution and mechanical properties is important for the development of reasonable thermomechanical processing route and improving the performance of titanium alloys.

It has been widely accepted that dynamic globularization and static globularization are two grain refinement ways for titanium alloys, which occur in hot deformation and heat treatment, respectively[9]. Dynamic globularization is controlled by boundary splitting mechanism, that is, the β phase penetrates α grain along the boundaries, resulting in dynamic recrystallization (DRX)[10,11]. Generally, the dynamic globularization of lamellar α phases involves a series of microscopic processes. Specifically, with the action of hot deformation, the semi-coherent Burgers vector relationship (BOR) between α and β phase may be broken, and the low angle sub-boundaries form in the acicular α grains, which will further change to the high angle boundaries[12]. Finally, the lamellar α grains can be successfully fragmentized into the fine grains under the actions of interfacial tension and element diffusion[13,14]. The static globularization is realized in the process of static recrystallization (SRX) or recrystallization annealing. SRX

Received date: December 26, 2020
Foundation item: National Natural Science Foundation of China (51871242); National Key R&D Program of China (2018YFB0704100); Key R&D Program of Hunan Province, China (2016JC2003)
Corresponding author: Zhang Xiaoyong, Ph. D., State Key Laboratory of Powder Metallurgy, Central South University, Changsha 410083, P. R. China, Tel: 0086-731-88830464, E-mail: zhangxiaoyong@csu.edu.cn

plays a significant role in grain refinement for both α and β phase [15,16].

Hot rolling is one of the commonly used manufacturing methods for titanium alloy plate and tube, which is very effective in improving microstructures and properties[17,18]. For instance, hot rolling can cause a large plastic deformation and change grain shape and size[19-21], and subsequent heat treatment can lead to SRX and fine phase precipitation[22,23]. Wang et al[24] proposed that the equiaxed α grain is elongated along the rolling direction during hot rolling, and then an equiaxed morphology is formed during annealing in TC21 alloy. The intensity of microtexture is increased by the oriented arrangement of deformed grains[25]. Li et al[26] investigated the lamellar α evolution of Ti-55511 alloy during isothermal deformation, and then found that the fragmentation of lamellar α preferentially occurs at the α/α subgrain boundary through β penetration. Jia et al[27] proposed that the stress relaxation can effectively induce the spheroidization of residual lamellar α phase in Ti-7333 alloy. The occurrence of DRX usually needs large deformation and proper temperature during hot deformation[28,29]. Lin et al[30] investigated the phase transformation and dynamic recrystallization behavior in Ti-55511 alloy during hot compression and found that DRX degree enhances with raising the deformation degree or decreasing the strain rate. Liu et al[31] investigated effect of annealing on microstructure and properties of titanium alloy, and found that annealing temperature affects grain size and morphology distribution. The effect of annealing temperature on microstructure evolution is complex. On the one hand, the increasing annealing temperature promotes the grain refinement. On the other hand, an excessively high temperature causes the apparent transformation from α to β phase, which results in a large decrease of α content and an apparent coarsening of β grain, then harming the comprehensive properties[32]. In addition, the hot rolling temperature is also an important parameter affecting microstructure evolution, and the $\alpha+\beta$ rolled Ti-3.5Al-5Mo-6V-3Cr-2Sn-0.5Fe alloy shows smaller β grain size than β rolled alloy in all heat treatment conditions[33].

However, current research mainly focuses on spheroidization of lamellar α, and there are few reports comparing microstructure evolution and mechanical properties of Ti-55511 alloys with equiaxed and lamellar microstructures during thermomechanical processing. Meanwhile, it has been well accepted that the study of texture evolution and its influence on mechanical properties play a vital role in keeping performance consistency. Systematic investigation about anisotropy and microstructure evolution is limited, which subsequently confines a fundamental understanding about the effect of thermomechanical processing on the microstructure evolution and anisotropy.

Therefore, this work mainly aims to explore the microstructure evolution and mechanical properties of equiaxed and lamellar Ti-55511 alloy during hot rolling and annealing. Firstly, the mechanical properties of Ti-55511 were obtained by tensile test. Secondly, microstrucural characteristics were investigated by methods of scanning electron microscopy (SEM) and electron backscattered diffraction (EBSD). Specific attention was paid on different microstructure evolution and deformation mechanism by combination of inverse pole figure (IPF) and transmission electron microscope (TEM). Then, the fracture surface and crack observation were used to explain the anisotropy.

1 Experiment

The raw material was forged bar with Φ150 mm provided by Hunan Goldsky Titanium Industry Technology Co., Ltd. The chemical compositions (wt%) were Al-5.20, Mo-4.92, V-4.96, Cr-1.05, Fe-0.96 and balance Ti. The $\beta/\alpha+\beta$ transus temperature was approximately 875±5 °C, measured by traditional metallographic method. The as-received microstructure of forged Ti-55511 bar contains nearly equiaxed primary α, fine secondary α and β matrix, as illustrated in Fig.1a.

The 80 mm×35 mm×15 mm billets were lineally cut from the forged bar, and then placed into a quartz tube furnace. Two heat treatment routes (Fig. 1b) were carried out to obtain the equiaxed and lamellar microstructures: (1) heating at 750 °C for 60 min followed by water quenching; (2) solution treatment at 920 °C for 30 min and water quenching, followed by aging at 710 °C for 120 min and water quenching.

As illustrated in Fig. 1c, the equiaxed microstructures still include some fine secondary α phases and have no β grain boundaries, while the lamellar microstructures contain triangularly distributed lamellar α with 2~3 μm in length and 0.2~0.5 μm in width (Fig. 1d). The billets with the equiaxed and lamellar microstructures were kept at 750 °C for 30 min and then hot rolled in LO-500 rolling mill. The total rolling reduction was 80% (from 15 mm to 3 mm), and per pass reduction was 8%. In order to keep the rolling temperature, the as-rolled samples were placed into a muffle furnace for 3 min after each pass. After final pass, samples were water quenched, followed by annealing at 600 °C for 1 h and water quenching. The tensile samples were lineally cut along rolling direction (RD) and transverse direction (TD) from the final rolled and annealed samples, respectively.

SEM samples were prepared by mechanical grinding, polishing, etching with Kroll reagent (1.5 mL HF+3 mL HNO_3+100 mL H_2O) and ultrasonic cleaning with absolute ethanol. SEM observation was carried on Quanta FEG 250 scanning electron microscope with backscatter mode. EBSD and TEM samples were prepared by mechanically thinning, punched into Φ8 mm disc and twin-jet electropolishing with electrolyte (300 mL methanol+175 mL n-butanol+25 mL perchloric acid). EBSD observation was performed on Helios NanoLab G3 UC focused ion/electron dual beam field emission scanning electron microscope, and EBSD data was analyzed by TSL-OIM software. TEM observation was employed by JEM-2100F field emission transmission electron microscope with speed voltage of 200 kV. Room temperature tensile tests were conducted by Instron 3369 testing machine with a speed of 1 mm/min, and every test was repeated three times.

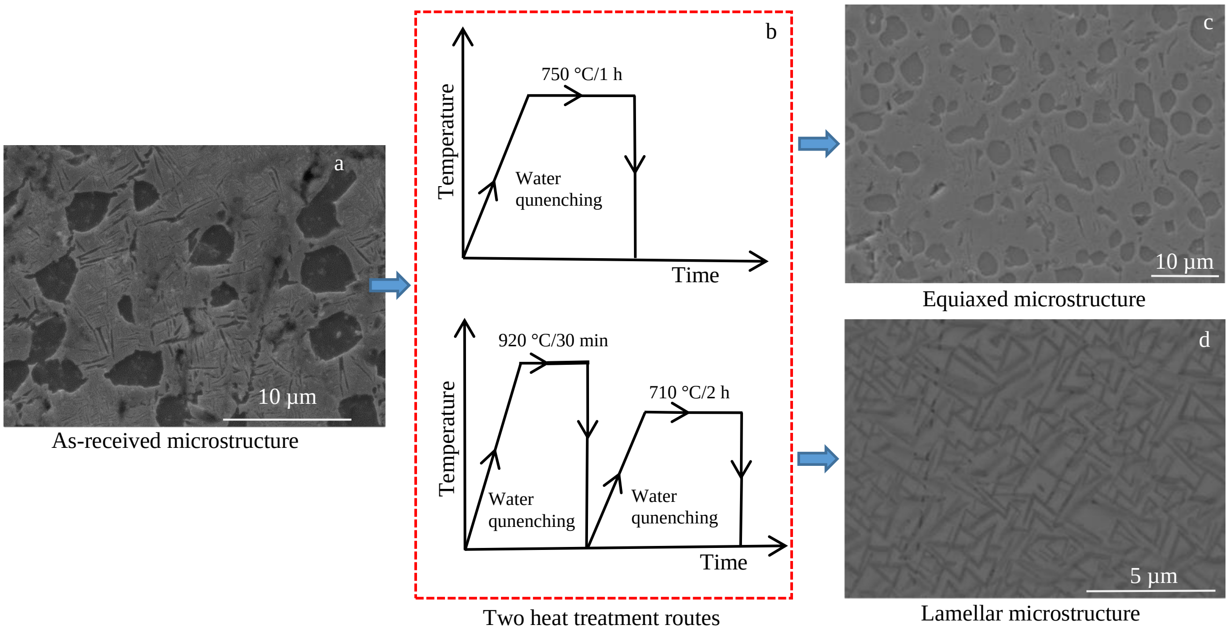

Fig.1 Initial microstructure (a) and two types of heat treatment routes (b) to obtain equiaxed (c) and lamellar (d) microstructures

2 Results

2.1 Microstructure

Fig. 2 displays the microstructures of Ti-55511 in normal direction-rolling direction (ND-RD) plane after 750 °C rolling and 600 °C annealing. The morphology of *α* phase shows a slight elongation along rolling direction in the hot rolled sample with equiaxed structure, and *α* phase size has no obvious change. The length and width of *α* phase are about 8 and 3 μm, respectively. Meanwhile, the fine lamellar *α* phase in the initial microstructure (Fig. 1c) almost disappears completely (Fig. 2a). After 600 °C annealing, the spheroidization of *α* phase produces nearly equiaxed *α* grains with an average diameter of 4 μm, and many secondary *α* grains precipitate in *β* matrix (Fig.2b).

However, the lamellar *α* grains have significant deformation and are generally distributed along the same directions during hot rolling (Fig. 2c). Meanwhile, some *α* grains are bent,

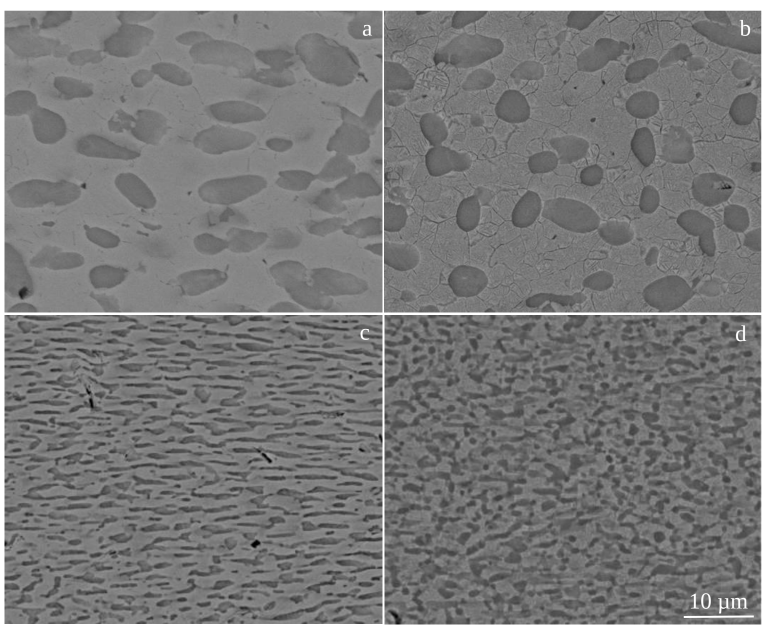

Fig.2 Microstructures of Ti-55511 with equiaxed (a, b) and lamellar (c, d) structures in ND-RD plane after 750 °C rolling and 600 °C annealing: (a, c) hot-rolled and (b, d) annealed

twisted and fragmentized into fine equiaxed α grains. Considering that the rolling mode is unidirectional and loading condition is relatively simple, lamellar α grain cannot be completely broken. Fig.2d shows that primary α grain gets significantly shortened. Comprehensively, the morphology of α grains in lamellar structures significantly changes after hot rolling and annealing.

In order to further understand microstructure evolution and softening mechanism of Ti-55511 alloy with equiaxed and lamellar structures during hot rolling, EBSD and TEM observations were conducted. Fig.3 shows IPFs of Ti-55511 alloy with equiaxed and lamellar structure after 750 °C rolling, in which white lines (pointed by the green arrow) represent low angle grain boundaries (misorientation angle: 2°~15°), black lines (pointed by the black arrow) refer to high angle grain boundaries (misorientation angle: >15°). EBSD provides quantitative measurements of corresponding misorientation distribution after hot rolling. Fig.4 shows the misorientation distribution of grain boundaries in the α and β phase. For equiaxed structure after rolling (shown in Fig. 3a and 3b, Fig.4a and 4b), there are mainly low angle grain boundaries inside the α grains, while interior of β matrix both has low angle grain boundaries and high angle grain boundaries. It is notable that some recrystallized new β grains in Fig.3b appear in local regions, indicating that β matrix has already generated dynamic recrystallization. For lamellar structures after rolling (shown in Fig. 3c and 3d and Fig.4c and 4d), interior of α grains both contains low angle grain boundaries and high angle grain boundaries, and interior of β matrix only consists of low angle grain boundaries. Meanwhile, lamellar α grains are surrounded with some fine equiaxed α grains, suggesting that some lamellar α grains have already fragmentized, as shown in Fig.3c.

Fig.5 shows the TEM micrographs of Ti-55511 alloy with equiaxed structure and lamellar structure after 750 °C rolling, and white lines represent grain boundaries between α and β phase. The equiaxed α phase is elongated in hot rolled samples (Fig. 5a), and lots of dislocations (Fig. 5b) are accumulated at α/β interfaces and β matrix. Meanwhile, β subgrain boundary is clearly seen in β matrix (Fig.5b), which further proves that β matrix has dynamic recovery and dynamic recrystallization. Crossing twins are observed in the elongated α grain (Fig. 5c). It is confirmed that the crossing twinning belongs to $\{1\bar{1}01\}$ twinning system and has two variants in α grains[29]. It is shown that two variants are generated in the elongated α phase (selected area electron diffraction (SAED) pattern along the $[1\bar{2}1\bar{3}]_\alpha$ zone axis, Fig. 5d). After rolling deformation, the lamellar α is bent (Fig.5f), and the middle of lamellar α grain has a V-groove. Part of the β-matrix is wedged in the lamellar α, and part of the β-matrix penetrates the lamellar α, which means that lamellar α has been dynamically spheroidized into equiaxed α.

2.2 Microtexture

Besides the microstructure evolution, microtexture in Ti-55511 alloy with equiaxed and lamellar structure also changes obviously after hot rolling and annealing. Fig. 6 shows the microtexture of Ti-55511 alloy with equiaxed structure during 750 °C rolling and 600 °C annealing. The $(0001)_\alpha$ pole of equiaxed structure is more dispersed and partially corresponds to the $(110)_\beta$ pole, as shown in Fig.6a and 6d, indicating that there is no perfect BOR between α phase and β matrix. The maximum texture intensities of α and β phases are 10.1 and 21.9, respectively. Compared with Fig. 6a and 6d, the distribution of $(0001)_\alpha$ pole (Fig.6b) and $(110)_\beta$ pole (Fig.6e) in hot-rolled sample changes, texture intensity of α phase increases slightly from 10.1 to 17.1, and texture intensity of β

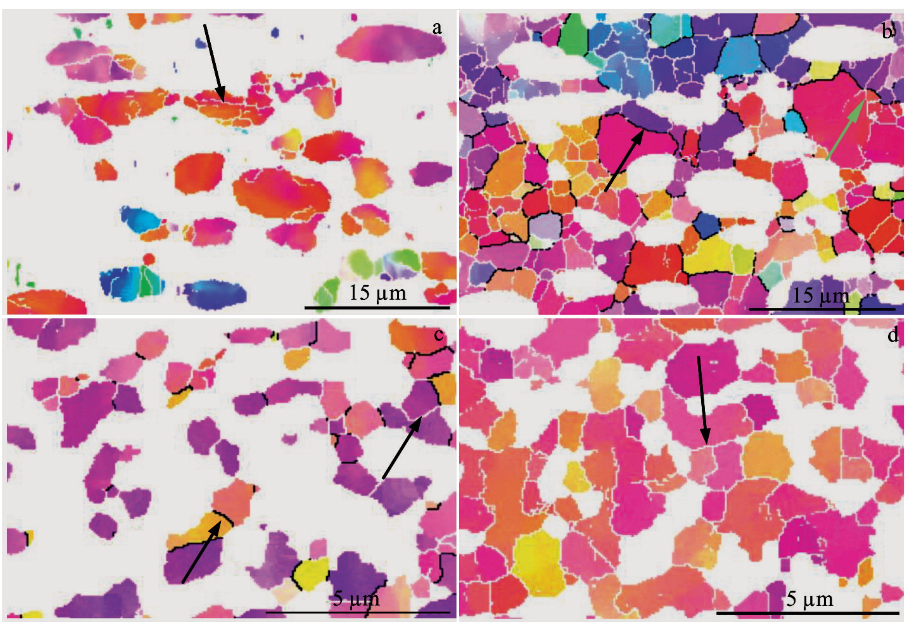

Fig.3 IPFs of rolled Ti-55511 samples with equiaxed structure (a, b) and lamellar (c, d) structures: (a, c) α phase and (b, d) β phase

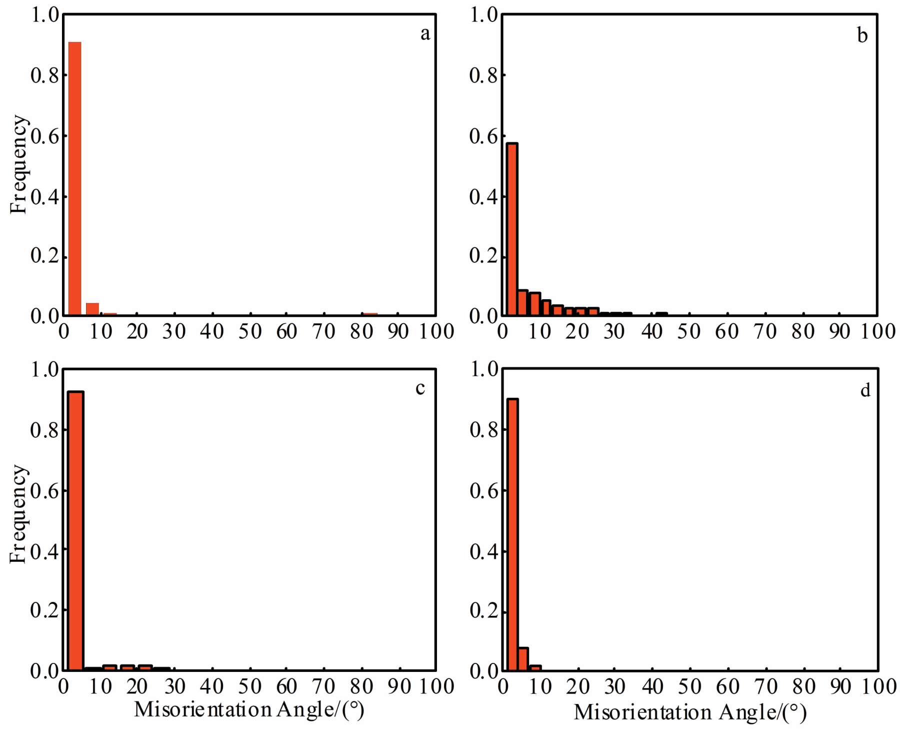

Fig.4 Misorientation distribution of rolled Ti-55511 samples with equiaxed structure (a, b) and lamellar (c, d) structures: (a, c) α phase and (b, d) β phase

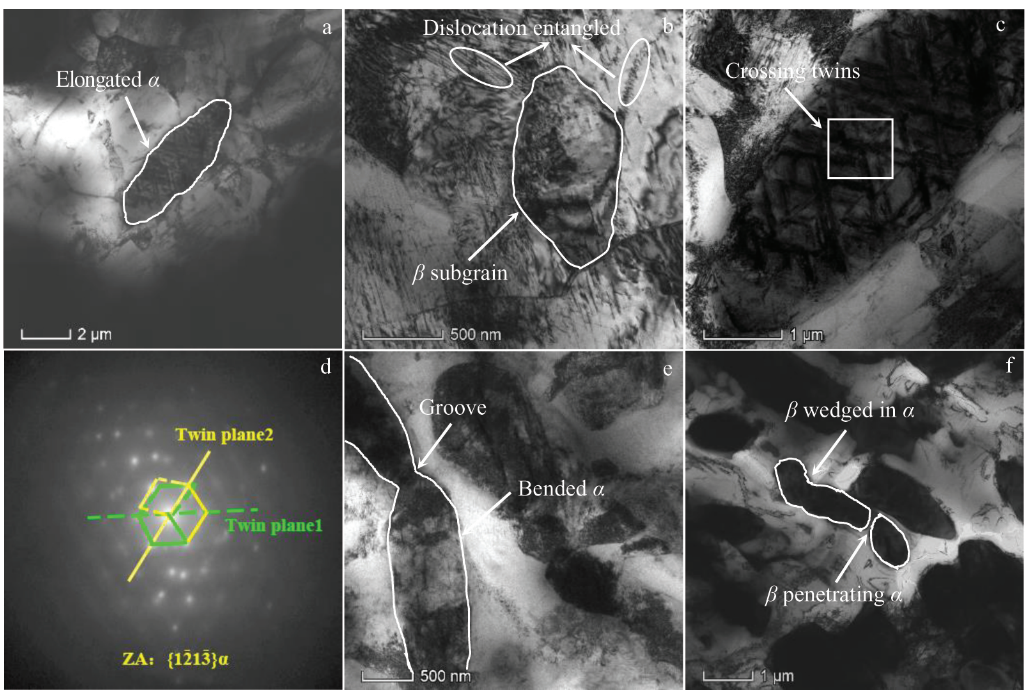

Fig.5 TEM images showing deformation characteristics in hot rolled sample: (a) elongated α in rolled sample with equiaxed structure; (b) dislocations and β subgrain in rolled sample with equiaxed structure; (c) twinning in elongated α in Fig.5a; (d) SAED pattern along the $[11]_{\alpha}$ zone axis revealing crossing twins identified as two twin variants; (e) bended α and groove in rolled sample with lamellar structure; (f) β wedged in α and β penetrating α

phase decreases from 21.9 to 12.1. After annealing, the distribution of $(0001)_{\alpha}$ pole (Fig.6c) and $(110)_{\beta}$ pole (Fig.6f) in annealed sample also changes. The distribution of $(0001)_{\alpha}$ pole is more dispersed, while the distribution of $(110)_{\beta}$ pole is

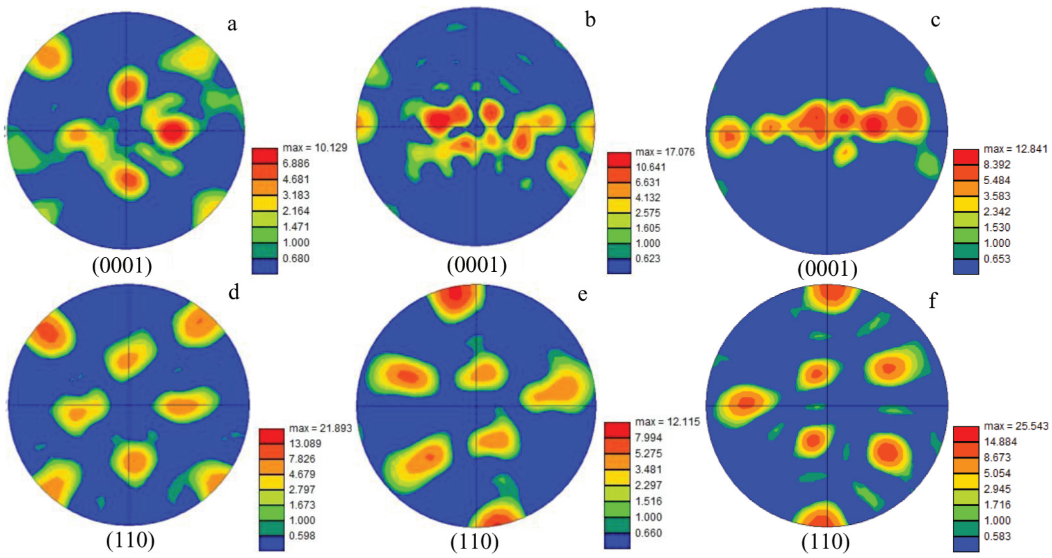

Fig.6 Microtextures of Ti-55511 alloy with equiaxed structure: (a, d) equiaxed sample, (b, e) rolled sample, and (c, f) annealed sample

more concentrated. Therefore, the texture intensity of α phase decreases slightly from 17.1 to 12.8, and texture intensity of β phase increases from 12.1 to 25.5.

Fig. 7 shows the microtexture of Ti-55511 alloy with lamellar structure during 750 °C rolling and 600 °C annealing. The $(0001)_\alpha$ pole of lamellar structure is intensively distributed, and completely corresponds to the $(110)_\beta$ pole, as shown in Fig.7a and 7d, indicating that α phase keeps perfect Burgers vector relationship with β matrix, i. e. $\{0001\}_\alpha//\{110\}_\beta$. The maximum texture intensities of α and β phase are 24.4 and 39.9, respectively. Compared with Fig. 7a and 7d, the distribution of $(0001)_\alpha$ pole (Fig. 7b) in hot-rolled sample changes significantly, implying that the BOR between α and β phase is destroyed during hot rolling process. Meanwhile, the distribution of $(110)_\beta$ pole (Fig.7e) in hot-rolled sample has no obvious change. The texture intensity of α phase increases obviously (maximum value increases from 24.4 to 54.6), and the maximum texture intensity of β phase slightly decreases from 39.9 to 37.6. After annealing, the peak number of $(0001)_\alpha$ pole (Fig. 7c) in annealed sample increases, while the distribution of $(110)_\beta$ pole (Fig. 7f) changes and is more dispersed. The maximum texture intensities of α change from 54.6 to 12.3 and that of β phase change from 37.6 to 25.7, which can be ascribed to the precipitation of secondary α grains.

2.3 Mechanical properties

As illustrated in Fig. 8, the mechanical properties of Ti-55511 alloy with equiaxed and lamellar structures are compared after 750 °C rolling and 600 °C annealing. The ultimate tensile strength (UTS) and elongation (EL) along RD

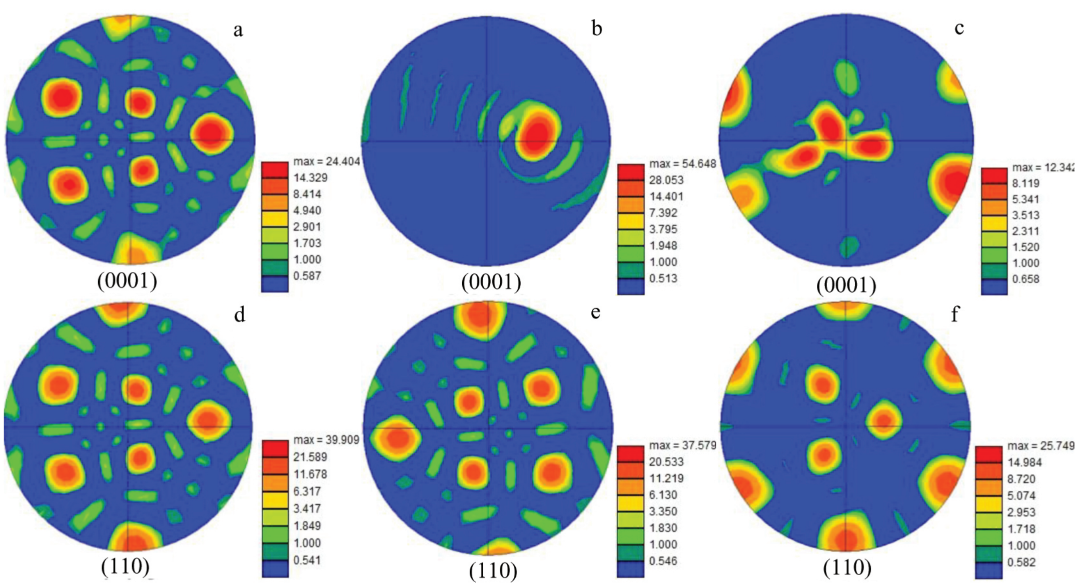

Fig.7 Microtextures of Ti-55511 alloy with lamellar structure: (a, d) acicular sample, (b, e) rolled sample, and (c, f) annealed sample

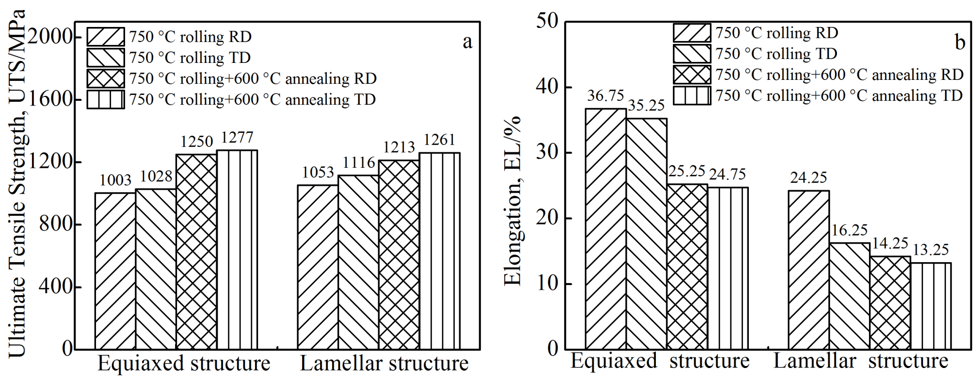

Fig.8 Comparison of mechanical properties between equiaxed and lamellar structures: (a) ultimate tensile strength and (b) elongation

and TD of equiaxed structure after hot rolling are 1003 and 1028 MPa, 36.75% and 35.25%, respectively. After further annealing at 600 °C, UTS along RD and TD increases to 1250 and 1277 MPa, while EL along RD and TD decreases to 25.25% and 24.75%, respectively. It can be found that its anisotropy of mechanical properties between RD and TD is not obvious after hot-rolling and annealing. As for the lamellar structure, UTS along RD and TD are 1053 and 1116 MPa (after hot rolling), 1213 and 1261 MPa (after annealing), respectively, which shows the obvious anisotropy. EL is 24.25% (RD) and 16.25% (TD) after hot rolling, which also shows the obvious anisotropy. However, after further annealing, El and its anisotropy are reduced, and EL is 14.25% (RD) and 13.25% (TD).

2.4 Fracture morphology

The tensile fractured surfaces of equiaxed structure after rolling and annealing along RD and TD were analyzed to further study the mechanical properties. Dense and homogenous dimples with an average size of about 10 μm are abundant in hot-rolled specimen along RD (Fig. 9a) and TD (Fig. 9b), in which the fracture mode can be considered as a ductile fracture. In addition to some small holes in Fig. 9b, the difference of tensile fractured morphology along RD and TD is not obvious, indicating that tensile plasticity along RD and TD is good and have little difference. Many uniform dimples with average size of about 4 μm and shallower depth are still distributed in the SEM image of annealed specimen RD (Fig. 9c) and TD (Fig. 9d). After annealing, the tensile plasticity along RD and TD of the sample is reduced, which is consistent with the mechanical properties test results.

Fig. 10 shows the fracture surfaces of lamellar α structure after 750 °C hot rolling and 600 °C annealing, and the samples are stretched along RD (Fig. 10a and 10c) and TD (Fig. 10b and 10d). From Fig.10a and 10b, many dense shallow dimples with a size of about 8 μm can be observed in tensile fracture along RD, while distinct facets appear in tensile fracture along

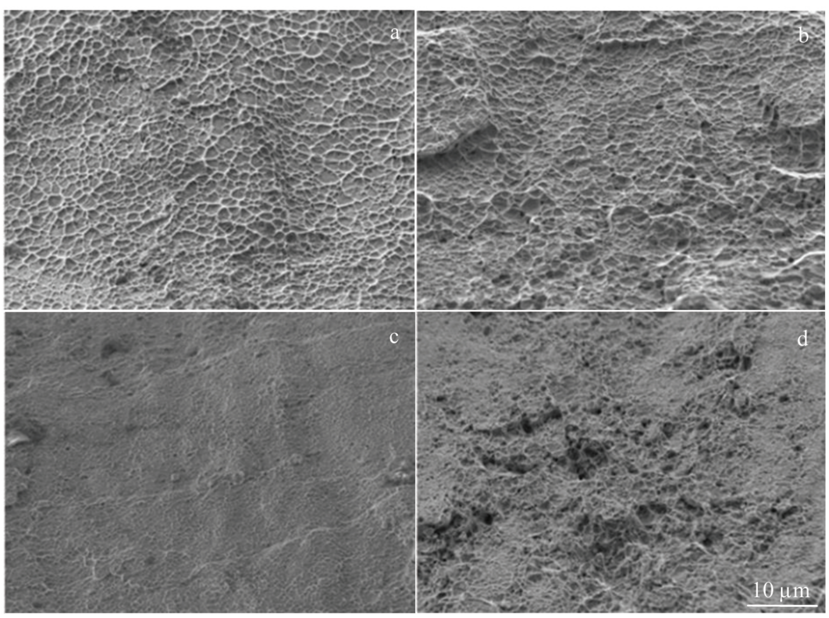

Fig.9 SEM morphologies of fracture surfaces of equiaxed Ti-55511 after rolling (a, b) and annealing(c, d): (a, c) RD and (b, d) TD

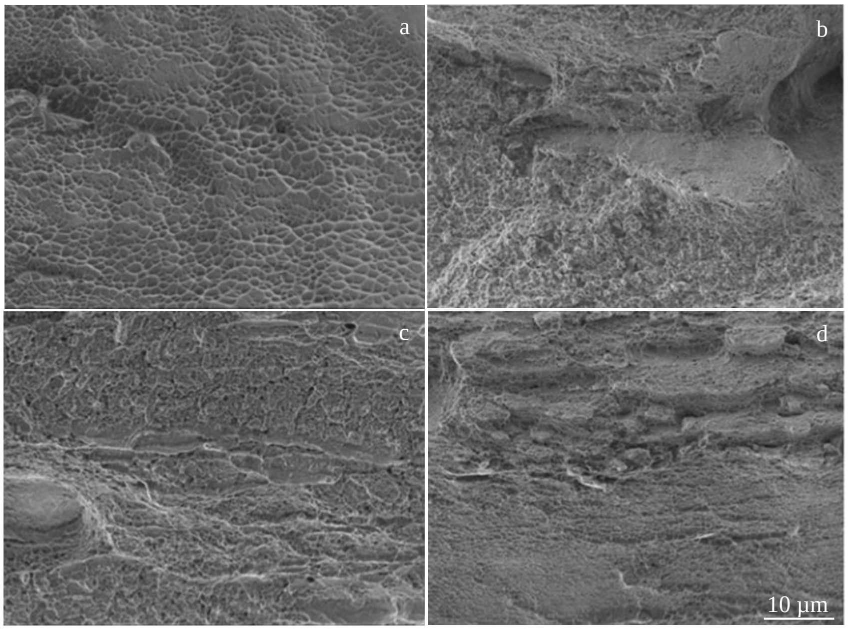

Fig.10 Fracture surface morphologies of lamellar Ti-55511 after rolling (a, b) and annealing (c, d): (a, c) RD and (b, d) TD

TD, which implies that tensile plasticity along RD is higher than along TD. Compared with Fig. 10a and 10b, distinct facets and fine dimples can be both observed in samples after annealing along RD and TD (shown in Fig. 10c and 10d), which indicates that the ductilities of both samples decrease owing to the annealing process. The reason can be explained by the precipitation of secondary α phases during the 600 °C annealing, which provides more microcrack sites.

3 Discussion

Different mechanical properties between equiaxed and lamellar microstructures should be related to different microstructure evolutions. For equiaxed structure, secondary α is dissolved back, which are considered to be the action of stress field and temperature field after hot rolling. However, after annealing, the secondary fine α precipitates and forms dispersion strengthening, which leads to the increase of strength and decrease of plasticity. During the process of deformation and heat treatment, there is no obvious morphological change and no obvious directional arrangement of the equiaxed α phase. The anisotropy of tensile mechanical properties of equiaxed α structure after rolling and annealing is very slight.

After hot rolling of lamellar microstructure, the α phases have undergone significant deformation and are generally broken into fine equiaxed α grains (Fig. 2c and Fig. 3c). This deformation mechanism is called dynamic spheroidization. On the one hand, the difference about interfacial tension between center and ends in α grains causes element migration to shorten the width of α grains. On the other hand, the bigger nucleation driving force makes many secondary α grains precipitate in β matrix. The spheroidization of lamellar α phase can refine the original α grains. At the same time, grain boundary of α transforms into a high angle grain boundary after annealing, which fragmentizes during the β wedging process. Many secondary α grains are precipitated in β matrix. As for lamellar α structure, the increase of strength and the decrease of plasticity are owing to spheroidization of primary α and precipitation of secondary α. It is thought that there are two strengthening mechanisms, namely the fine grain strengthening and second phase dispersion strengthening [34]. After hot rolling, the lamellar α phase rotates obviously and forms a directional arrangement. The spheroidization degree of α phase varies in different orientations, because the degree of difficulty of crack propagation is different in all directions. Therefore, the plastic anisotropy of lamellar structure after rolling is relatively significant. After annealing, α phase is further spheroidized, and its size in RD and TD directions is more similar. Consequently, the plastic anisotropy of lamellar structure after annealing decreases.

Comparing the strength and plasticity of equiaxed and lamellar structure, the equiaxed structure strength after hot rolling is lower than that of the lamellar structure. The lamellar α is fragmentized to a certain extent and the grains are refined. While, the equiaxed α phase is almost never broken after hot rolling. After annealing, a large number of fine, dispersed secondary α phases are precipitated from equiaxed structure. But, there is less secondary α precipitates from lamellar structure. Therefore, the equiaxed structure strength after annealing is higher than that of lamellar structure. The size of the equiaxed α phase is larger than that of the acicular α phase, which has a larger effect on the crack growth. The plasticity of equiaxed structure is higher than that of lamellar structure, whether it is rolled or annealed.

In summary, it can be concluded that mechanical properties of Ti-55511 alloy with equiaxed and lamellar structures after

750 °C rolling and 600 °C annealing are related to microstructure and microtexture evolution. For Ti-55511 alloy with equiaxed structure, equiaxed α grains show a slightly directional elongation under the action of hot rolling, which causes the increase of α phase texture intensity. Equiaxed α grains do not keep perfect BOR with β matrix, which can offer large deformation resistance. Meanwhile, the large deformation distortion energy makes β matrix generate dynamic recrystallization. It is confirmed that interior of β matrix both has low angle grain boundaries and high angle grain boundaries, and some new fine β grains are found (Fig. 3b). DRX causes an obvious decrease in the texture intensity of β phase. For hot-rolled Ti-55511 with equiaxed structure after 600 °C annealing, many fine secondary α grains uniformly precipitate and β grains grow. Therefore, the texture intensity of α phase decreases slightly and texture intensity of β phase increases.

For Ti-55511 alloy with lamellar structure after rolling, lamellar α grains that maintain a perfect BOR with β matrix can easily rotate to a special orientation and partly fragmentize, which makes texture intensity of α grains significantly increase and consumes most of distortion energy. Residual distortion energy cannot lead to the occurrence of dynamic recrystallization in β matrix. In other words, β matrix only generates dynamic recovery, which further causes texture intensity of β phase to decrease slightly. After 600 °C annealing, the recrystallization of β grains results in the further weakening of texture. Enough nucleation driving force makes many secondary α grain uniformly precipitate in β matrix, which causes the decrease of texture intensity of α phase and finally diminishes the anisotropic mechanical properties.

4 Conclusions

1) During 750 °C rolling of Ti-55511 alloy, α grain in equiaxed structure is slightly deformed, β phase undergoes dynamic recovery and dynamic recrystallization, and some new β grains are formed in local region. The texture intensity of α phase becomes slightly enhanced, and the texture intensity of β phase gets slightly weakened. After 600 °C annealing, the texture intensity of α phase decreases slightly, while texture intensity of β phase increases.

2) During 750 °C rolling, morphology of α grain in lamellar structure changes significantly, some of which are bent, twisted and fragmentized. Meanwhile, dynamic recovery takes place in β phase. The texture intensity of α phase is significantly enhanced and the texture intensity of β phase is slightly reduced. After 600 °C annealing, the number of equiaxed α grains increases, β matrix is distributed with lots of secondary α grains, and the texture intensity of α and β phase both decreases.

3) The anisotropy of mechanical properties in equiaxed structure after 750 °C rolling and 600 °C annealing is very slight, and the anisotropy of mechanical properties in lamellar structure after rolling at 750 °C is relatively significant. After 600 °C annealing, the anisotropy of mechanical properties in lamellar structure decreases.

References

1 Chen W, Li C, Zhang X Y *et al*. *Journal of Alloys and Compounds*[J], 2019, 783: 709

2 Qu F S, Zhou Y H, Zhang L Y *et al*. *Materials & Design*[J], 2015, 69: 153

3 Banerjee D, Williams J C. *Acta Materialia*[J], 2013, 61(3): 844

4 Boyer R R, Briggs R D. *Journal of Materials Engineering and Performance*[J], 2013, 22(10): 2916

5 Chen W, Lv Y P, Zhang X Y *et al*. *Rare Metal Materials and Engineering*[J], 2020, 49(3): 897 (in Chinese)

6 Sadeghpour S, Abbasi S M, Morakabati M *et al*. *Materials & Design*[J], 2017, 121: 24

7 Tarzimoghadam Z, Sandlobes S, Pradeep K G *et al*. *Acta Materialia*[J], 2015, 97: 291

8 Lütjering G. *Materials Science and Engineering A*[J], 1998, 243(1): 32

9 Stefansson N, Semiatin S L. *Metallurgical and Materials Transactions A*[J], 2003, 34(3): 691

10 Dai Y, Lv Y P, Li S J *et al*. *Rare Metal Materials and Engineering*[J], 2019, 48(4): 1109

11 Weiss I, Froes F H, Eylon D *et al*. *Metallurgical and Materials Transactions A*[J], 1986, 17(11): 1935

12 Klimova M, Zherebtsov S, Salishchev G *et al*. *Materials Science and Engineering A* [J], 2015, 645: 292

13 Semiatin S L, Seetharaman V, Weiss I. *Materials Science and Engineering A* [J], 1999, 263(2): 257

14 He D, Zhu J C, Lai Z H *et al*. *Materials & Design*[J], 2013, 46: 38

15 Sharma G, Ramanujan R V, Tiwari G P. *Acta Materialia*[J], 2000, 48(4): 875

16 Wang K, Li M Q, Liu Q. *Materials Characterization*[J], 2016, 120: 115

17 Dong R F, Li J S, Zhou H C *et al*. *Materials Characterization*[J], 2017, 129: 135

18 Sun J F, Zhang Z W, Zhang M L *et al*. *Journal of Alloys and Compounds*[J], 2016, 663: 769

19 Murty S V S N, Nayan N, Kumar P *et al*. *Materials Science and Engineering A*[J], 2014, 589: 174

20 Chen Y, Li J S, Tang B *et al*. *Journal of Alloys and Compounds* [J], 2015, 618: 146

21 Warchomicka F, Poletti C, Stockinger M. *Materials Science and Engineering A*[J], 2011, 528(28): 8277

22 Matsumoto H, Kitamura M, Li Y *et al*. *Materials Science and Engineering A*[J], 2014, 611: 337

23 Zhang X Y, Mei Y P, Lv Y P *et al*. *Metals*[J], 2018, 8(11): 904

24 Wang K, Wu M, Yan Z *et al*. *Journal of Alloys and Compounds* [J], 2018, 752: 14

25 Chen W, Lv Y P, Zhang X Y *et al*. *Materials Science and Engineering A*[J], 2019, 758: 71

26 Li C, Zhang X Y, Li Z Y *et al*. *Materials Science and*

Engineering A[J], 2012, 558: 668
27 Jia C L, Kou H C, Chen N N *et al*. *Journal of Alloys and Compounds*[J], 2019, 781: 674
28 Liang H Q, Guo H Z, Ning Y Q *et al*. *Materials & Design*[J], 2014, 63: 798
29 Liang H Q, Guo H Z, NanY *et al. Materials Science and Engineering A*[J], 2014, 615: 42
30 Lin Y C, Huang J, He D G *et al*. *Journal of Alloys and Compounds*[J], 2019, 795: 471
31 Liu C M, Lu Y, Tian X J *et al*. *Materials Science and Engineering A* [J], 2016, 661: 145
32 Shi R, Li G J, Xia Y M *et al*. *Journal of Alloys and Compounds* [J], 2017, 705: 183
33 Du Z X, Xiao S L, Shen Y P *et al*. *Materials Science and Engineering A*[J], 2015, 631: 67
34 Li C, Zhang X Y, Li Z Y *et al*. *Materials Science and Engineering A*[J], 2013, 573: 75

等轴和片层组织Ti-55511合金热轧及退火过程中的组织演变及力学性能

史双喜[1]，樊　凯[2]，杨　胜[2]，张晓泳[1]，周科朝[1]
(1. 中南大学 粉末冶金国家重点实验室，湖南 长沙 410083)
(2. 湖南金天钛业科技有限公司，湖南 常德 410007)

摘　要：锻态Ti-55511合金经过不同的热处理工艺，获得等轴和片层2种初始组织。采用SEM、EBSD、TEM和拉伸试验研究了等轴和片层Ti-55511合金在热轧和退火过程中的组织演变和力学性能。结果表明：经750 ℃轧制，等轴组织中的α相轻微变形，β相发生动态回复和动态再结晶；而片层组织中的α相几乎平行分布，有些部分破碎，β相仅产生动态回复。等轴组织中的α相织构强度略有增加，片层组织中α相织构强度显著增加；而等轴和片层组织中β相织构强度均降低。同时，等轴组织力学性能各向异性很小，片层组织各向异性明显。600 ℃退火后，片层组织的α和β相织构强度均降低，力学性能的各向异性显著降低。

关键词：Ti-55511合金；动态回复；动态再结晶；组织演变；织构

作者简介：史双喜，男，1983年生，博士，中南大学粉末冶金国家重点实验室，湖南 长沙 410083，电话：0731-88830464，E-mail：shishxi2019@csu.edu.cn